Unsteady Flow Modeling of Pressure Real-Time Control in Water Distribution Networks

Enrico Creaco[1]; Alberto Campisano[2]; Marco Franchini[3]; and Carlo Modica[4]

Abstract: This paper investigates the potential of unsteady flow modelling for the simulation of remote real-time control (RTC) of pressure in water distribution networks. The developed model combines the unsteady flow simulation solver with specific modules for generation of pulsed nodal demands and dynamic adjustment of pressure control valves in the network. The application to the skeletonized model of a real network highlights the improved capability of the unsteady flow simulation of RTC compared with the typical extended period simulation (EPS) models. The results show that the unsteady flow model provides sounder description of the amplitude of the pressure head variations at the controlled node. Furthermore, it enables identification of the suitable control time step to be adopted for obtaining a prompt and effective regulation. Nevertheless, EPS-based models allow consistent estimates of leakage reduction as well as proper indications for valve setting under network pressure RTC at a much smaller computational cost. **DOI: 10.1061/(ASCE)WR.1943-5452.0000821.** © *2017 American Society of Civil Engineers.*

Author keywords: Control valves; Hydraulic transients; Water demand; Feedback control; Demand pulses; Water distribution systems; Real time control.

Introduction

Active control of pressures in water distribution networks (WDNs) is considered to be one of the more effective approaches to ensure correct delivery of drinking water to users with appropriate service levels (Farley and Trow 2003). Benefits of active pressure control include leakage reduction (Berardi and Giustolisi 2016; Vicente et al. 2016), which can be very crucial for communities experiencing water scarcity conditions.

Pressure control in WDNs typically is performed using pressure control valves (PCVs) with the aim to lead nodal pressure heads close to the lowest values that satisfy network user demand. Several single-objective (e.g., Vairavamoorthy and Lumbers 1998; Araujo et al. 2006; Liberatore and Sechi 2009; Ali 2015) and multiobjective (e.g., Nicolini and Zovatto 2009; Creaco and Pezzinga 2015a, b) optimization approaches have been proposed in order to identify the optimal locations of PCVs within WDNs. Most of these approaches require nodal demands to be provided as hourly or multihourly input to represent the time-varying network operation. The identification of optimal locations is followed by the selection of the valve type for appropriate pressure control. Traditional mechanical/hydraulic pressure reducing valves (PRVs) usually are adopted to enable the *local control* of the service pressure. These valves operate enforcing a *local* fixed pressure set point immediately downstream, irrespective of demand and service pressure variations in other nodes/areas of the network. Prescott and Ulanicki (2008) pointed out the possibility of improving operation of local PRV control through dynamic feedback control. Ulanicki and Skworcow (2014) identified the reasons why PRVs tend to oscillate at low flows and showed how this drawback can be solved by inserting a nonlinear compensator in the local control loop.

Various researchers recently have explored the potential for pressure control improvements by the introduction of remote real-time control (RTC) (e.g., Campisano et al. 2010, 2012; Creaco and Franchini 2013). Available studies highlight that remote RTC can be advantageous compared with local control of pressure. Remote RTC enables valves to be operated in real time as a function of remotely controlled nodes, which could feature the lowest pressure head in the network during the day. Therefore, in remote RTC, the valve closure is always adjusted to the largest possible value while respecting the minimum pressure constraint at the downstream nodes. This is beneficial compared with local PRV control, in which a single conservative setting is generally considered for the valve, thus leading, in general, to higher pressure heads and leakage downstream. Moreover, leakage is affected only by the average pressure signal; in fact, positive and negative pressure fluctuations compensate in terms of produced leakage (Campisano et al. 2016). Improved selection of the control nodes yields better service pressure regulation and larger leakage reductions (Creaco et al. 2016a). The remote RTC generally is carried out by dynamically adjusting the valve setting in order to keep the controlled pressure head close to the set point under variable demand conditions (Campisano et al. 2010). Remote RTC typically uses plunger or needle valves equipped with appropriate modules to support RTC (Svrcek et al. 2014), in which setting is easily modifiable in real time.

In the last decade, various RTC algorithms have been proposed and tested in WDN modelling. The first application of RTC for

[1]Assistant Professor, Dipartimento di Ingegneria Civile e Architettura, Univ. of Pavia, Via Ferrata 3, 27100 Pavia, Italy; Honorary Senior Research Fellow, College of Engineering, Mathematics and Physical Sciences, Univ. of Exeter, Prince of Wales Rd., Exeter EX4 4PL, U.K.; Adjunct Senior Lecturer, ~~and Faculty of Engineering, Computer and Mathematical Sciences~~, Univ. of Adelaide, Adelaide, SA 5005, Australia (corresponding author). E-mail: creaco@unipv.it

[2]Associate Professor, Dipartimento di Ingegneria Civile e Architettura, Univ. of Catania, Viale Andrea Doria 6, 95125 Catania, Italy. E-mail: acampisa@dica.unict.it

[3]Full Professor, Dipartimento di Ingegneria, Univ. of Ferrara, Via Saragat 1, 44100 Ferrara, Italy. E-mail: marco.franchini@unife.it

[4]Full Professor, Dipartimento di Ingegneria Civile e Architettura, Univ. of Catania, Viale Andrea Doria 6, 95125 Catania, Italy. E-mail: cmodica@dica.unict.it

Note. This manuscript was submitted on November 11, 2016; approved on April 14, 2017No Epub Date. Discussion period open until 0, 0; separate discussions must be submitted for individual papers. This paper is part of the ***Journal of Water Resources Planning and Management***, © ASCE, ISSN 0733-9496.

service pressure regulation in WDNs was carried out by Campisano et al. (2010), who used proportional control algorithms for regulating valve settings as a function of pressure measurements at controlled nodes. As a further development of their work, Campisano et al. (2012) proposed a dimensionless procedure for the calibration of these algorithms. Creaco and Franchini (2013) proposed a new control algorithm which enables a controlled pressure head to stay closer to the set point than the proportional controller. In addition to the pressure head measurement at the control node, this latter algorithm makes use of water discharge measurements at the valve site. Numerical simulations of RTC applications to real case studies were conducted by Berardi et al. (2015) and Campisano et al. (2016).

Although they are interesting contributions to the advance of knowledge in this research field, the previous works on remote RTC have the following limitations:

1. Nodal demands used for simulations were obtained in a simplified way, by multiplying the average daily demand by a time varying demand coefficient, which is linearized between two subsequent hours (Campisano et al. 2010, 2012; Creaco and Franchini 2013). A random noise eventually was superimposed to account for the stochastic nature of the demand (Campisano et al. 2016).
2. The WDN modelling was carried out under extended period simulation (EPS), in which the network operation is studied as a succession of steady states. This entails neglecting transient flow processes occurring in the network under RTC.

In order to overcome these limitations, this paper proposes a novel model structure to properly simulate the effects of RTC of nodal pressures in WDNs. The model enables taking account of the pulsed nature of demand as well as of the WDN hydraulic transients due to demand pulse triggering and to valve dynamic adjustments. Although the simulation of transients in WDNs has been widely investigated in the scientific literature (e.g., McInnis and Karney 1995; Jung and Karney 2009; Zhang et al. 2011; Nault and Karney 2016), the pulsed nature of demand generally is neglected and effects of transients associated with RTC of valves have been underexplored.

In the following sections, the model framework is described with specific reference to the pulsed demand generation at network nodes and to the unsteady flow modeling of the network under remote RTC of pressure control valves. The application to the skeletonised model of a real network follows. Results of the comparison of the unsteady flow modelling with EPS-based approaches also are highlighted.

Model Structure

Pulsed Demand Generation at Network Nodes

General Remarks

Pulse generation was used to reconstruct the demand at each network node. In this methodology, the pulse features in terms of arrivals τ (s), durations T (s), and intensities I (m^3/s) were generated as random variables following pre-fixed probability distributions. Specifically, the pulse arrivals were modeled as a nonstationary Poisson process (Buchberger et al. 2003). Although originally proposed for household demand generation, this approach can be extended to nodal demand generation in light of its scalability attribute (Buchberger et al. 2003). This attribute, which holds under conditions of uniform statistical properties of T and I, makes it possible to aggregate the pulse arrivals coming from the various homogeneous users connected to the same node. Therefore, for a certain node with N_h connected homogeneous users, if λ_i (s^{-1}) is the pulse arrival frequency associated with the ith connected user, the pulse arrival frequency λ (s^{-1}) of the node is additive across the users and can be calculated as $\sum_{i=1}^{N_h} \lambda_i$. If there are various categories of consumption at a certain node—that is, various groups of homogeneous users—pulse arrival frequencies must be summed separately for each category.

After the pulses produced by the generic network node have been generated, they can be aggregated at a certain temporal scale (e.g., 1 s, 1 h, and so forth). In particular, the total nodal demand at any time t (s) is obtained as the sum of intensities I of all the concurrent active pulses.

Mathematical Structure

In the pulse generation model, the time axis is traversed with a $\Delta\tau = 1$ s time step for each node. At a certain time t, the probability P of having exactly k pulses generated within the next time interval $\Delta\tau$ is

$$P(k) = e^{-\lambda\Delta\tau}\frac{(\lambda\Delta\tau)^k}{k!} \quad (1)$$

where parameter λ represents the pulse arrival frequency of the generic node. After sampling from Eq. (1) the number of pulses k produced at time t, each generated pulse is assigned arrival time $\tau = t$.

After defining pulse arrivals τ, values for T and I of the generic pulse are randomly generated using a bivariate probability distribution model (Creaco et al. 2015) in order to take account of the duration/intensity correlation. Creaco et al. (2015) used the bivariate lognormal distribution, which leads to values of T and I with lower bounds of zero and no upper bounds. In order to have both lower (T_{min} and I_{min}) and upper (T_{max} and I_{max}) bounds on T and I, the bivariate beta distribution is adopted in this case. The setup of this distribution requires nine parameters to be defined: the pulse duration–related parameters α_T, β_T, T_{min}, and T_{max}; the pulse intensity–related parameters α_I, β_I, I_{min}, and I_{max}; and correlation ρ between T and I.

Normally, the model described can be used to generate pulses of a long duration (e.g., 1 month) in which model parameters related to T and I can be assumed constant. Parameter λ, instead, varies based on a pattern aimed at describing daily variations in pulse arrivals, when the time axis is traversed with a time step of $\Delta\tau = 1$ s. Finally, one series of daily (24-h) consumption volumes can be constructed for each node. Because each nodal pulse is generated independently from the others, the series of daily nodal consumption volumes on a daily time step are expected to have mutual rank correlation equal to zero at the end of this process. Nevertheless, it is possible to re-sort the daily consumption volumes inside the series in order to preserve a certain lag0 rank correlation at daily time step, using the Iman and Canover (1982) method, for instance.

Parameterization

The parameterization of the pulse generation model would require for each network node the application of methodologies such as those proposed by Alvisi et al. (2003) and Creaco et al. (2016b). These methodologies involve searching for the model parameter values that lead to preservation of the statistical properties of consumption at various time aggregation scales at the same time. When no data are available for parameterization at a certain site, the following expeditious methodology, which consists of two steps, can be used.

In the first step, the nine parameters (α_T, β_T, T_{min}, T_{max}, α_I, β_I, I_{min}, I_{max}, and ρ) related to T and I can be derived through the

method of the moments (Hall 2004) on the basis of T and I data drawn from sites showing similar features to the site being modeled. In particular, the nine parameters can be obtained starting from estimates of $\bar{T}$, $\bar{I}$, σ_T, σ_I, $T_{\min}$, $I_{\min}$, $T_{\max}$, $I_{\max}$, and ρ, which represent the mean values of T and I, the standard deviations of T and I, the minimum values of T and I (normally set to 0), the maximum values of T and I, and the pulse duration/intensity correlation of the real pulses, respectively, observed in the reference time series.

In the second step, parameter λ is estimated in each node in such a way as to obtain the pre-fixed average nodal demand $\bar{D}$ in the day (m^3/s) for each demand category. This is done by enforcing the following condition, which expresses λ as the ratio of $\bar{D}$ to the average volume of the single pulse

$$\lambda = \frac{\bar{D}}{\bar{T}\,\bar{I} + \rho\sigma_T\sigma_I} \tag{2}$$

The pattern assigned to λ can be obtained starting from the pattern of the multiplying demand coefficient associated with the network area in which the generic node lies.

Unsteady Flow Modelling of WDNs

In the generic pipe of a WDN, the one-dimensional (1D) unsteady flow equations, which enable total head H (m) and water discharge Q (m^3/s) to be assessed along the pipes as a function of time, take on the following form derived from Wylie et al. (1993):

$$\frac{\partial H}{\partial x} + \frac{1}{gA}\frac{\partial Q}{\partial t} + J = 0$$
$$\frac{\partial H}{\partial t} + \frac{c^2}{gA}\frac{\partial Q}{\partial x} + \frac{c^2 q}{gA} = 0 \tag{3}$$

where x and t = abscissa along the pipe axis and time, respectively; A (m^2) = pipe cross-section area; and $g = 9.81$ m/s^2 is the gravity acceleration. The wave celerity c (m/s) can be calculated as

$$c = \left(\frac{\frac{\varepsilon}{\zeta}}{1 + \frac{\varepsilon D}{Es}}\right)^{1/2} \tag{4}$$

where ε (Pa) and ζ (kg/m^3) = water bulk modulus and density, usually set to 2.2×10^9 (at 4°C) and 1,000, respectively; E (Pa), D (m), and s (m) = pipe modulus of elasticity, diameter, and thickness, respectively. In Eq. (3), q (m^2/s) = outflow per unit of pipe length. This term can include leakage (Germanopoulos and Jowitt 1989), which can be calculated as a function of pressure head h (m) as

$$q = \alpha_{\text{leak}} h^{\gamma} \tag{5}$$

where α_{leak} ($m^{2-\gamma}/s$) and γ = leakage coefficient and exponent, respectively. Whereas γ depends on pipe material and crack shape (Van Zyl and Cassa 2014), α_{leak} depends on the number of cracks along the pipe and grows with pipe aging. Typically, α_{leak} is calibrated in order to obtain a prefixed leakage volume in the network in a certain time interval of network simulation.

In order to correctly represent the unsteady flow resistances in Eq. (3), the friction slope J is evaluated according to Pezzinga (2000) as

$$J = J_0 + k_p\left[\frac{\partial V}{\partial t} + c\,\text{sign}\left(V\frac{\partial V}{\partial x}\right)\frac{\partial V}{\partial x}\right] \tag{6}$$

where J_0 = resistance under steady flow conditions, which can be evaluated through such empirical uniform flow formulas as the Gauckler–Manning formula

$$J_0 = 10.29\frac{n^2|Q|Q}{D^{5.33}} \tag{7}$$

where n ($s/m^{1/3}$) = Gauckler–Manning coefficient.

Coefficient k_p (s^2/m) in Eq. (6) depends on pipe relative roughness and on the Reynolds number and energy friction losses under initial steady state conditions (Pezzinga 2000). However, for high Reynolds numbers, the dependence on the Reynolds number tends to vanish.

Unlike the work of Pezzinga (2000), which implemented a numerical method with staggered grid, this paper uses the method of the characteristics (Streeter et al. 1998) to solve Eq. (3) in order to derive H and Q in the inner cross sections of the generic pipe. This method discretizes the computational domain with finite spatial and temporal steps Δx and Δt and performs cubic interpolation of the variables along the spatial computation domain in order to have the same temporal step Δt in all the network pipes.

In order to obtain H and Q at either end node of the generic pipe, suitable boundary conditions are prescribed. Specifically, the head is assigned in the case of source node. In the case of the demanding node, the uniqueness of the head is considered. Additionally, the continuity equation is assigned, i.e., the sum of the water discharges entering the generic demanding node through the connected pipes equals the nodal outflow at each integration step. This paper considers the demand-driven modeling approach. The nodal outflow is assumed to be always equal to the nodal demand, which is evaluated in the section Pulsed Demand Generation at Network Nodes. In this context, the pressure-dependent effects on demand, which could be considered by means of equivalent opening areas along the pipe surface walls or at network nodes, are assumed to be negligible. This choice was made because the users generally regulate the tap opening in such a way as to obtain the desired outflow.

The unsteady flow modeling described was tested against network experimental observations carried out by Pezzinga (1999) under unsteady flow conditions generated by rapid valve closure. The results of such analyses (not reported in this paper) indicated a satisfactory fit of modelled water heads to the available data set of measurements.

In order to model the effects of control valves, the pipe fitted with the valve can be discretized with a single Δx. In order to represent suitably the head loss caused by the valve in the pipe in Eq. (3), J_0 in Eq. (7) is set as

$$J_0 = \frac{\xi|V|V}{2g\Delta x} \tag{8}$$

where V (m/s) = flow velocity in the pipe; and ξ = valve head loss coefficient, which is related to the valve closure setting α_v [0, 1] through relationships such as the following derived from Campisano et al. (2012):

$$\xi = 10^{c_1 - c_2\log_{10}(1-\alpha_v)} \tag{9}$$

where c_1 and c_2 are best-fit coefficients which can be evaluated from the $\xi(\alpha_v)$ curve provided by the valve manufacturer.

RTC Algorithm

The RTC algorithm implemented in this paper is algorithm LC2 proposed by Creaco and Franchini (2013). This control algorithm was chosen because the authors proved its robustness when WDN domestic demand changes during the year.

This algorithm enables regulation of a flow control valve in order to lead the pressure head h at the controlled node downstream

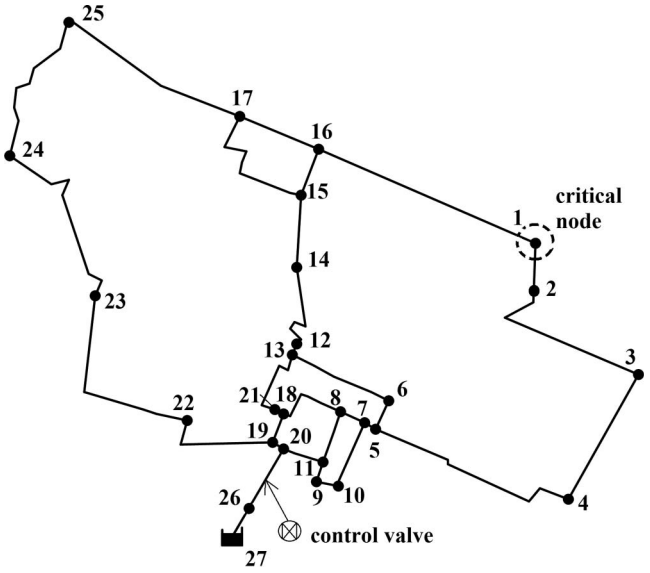

F1:1 **Fig. 1.** Network layout with node IDs; Critical Node 1 and control
F1:2 valve installed at the end of Pipe 32, with End Nodes 26 and 20

of the valve to the set-point value h_{sp}. The algorithm is based on measurement of deviation $e = h - h_{sp}$ and of flow velocity V in proximity to the valve.

At the generic time t (s), if Δt_{cont} (s) is the control time step (i.e., the period with which the regulation is performed) and if $\bar{e}$ and $\bar{V}$ are the average values of e and V, respectively, in the time interval $[t - \Delta t_{\text{cont}}, t]$, energy considerations lead to the following relationship for estimating the suitable valve setting correction $\Delta\alpha$:

$$\Delta\alpha(t) = 1 - \alpha(t) - 10^{\frac{c_1 - \log_{10}[K(\xi(t) + 2\, g\bar{e}/\bar{V}^2)]}{c_2}} \qquad (10)$$

where K = parameter that regulates the promptness of the control algorithm. Preliminary analyses showed that $K = 1$ is a good choice to obtain a sufficient degree of promptness, although the parameter can be finely tuned in order to maximize the algorithm performance, as was done by Creaco and Franchini (2013).

The $\Delta\alpha$ provided by Eq. (10) must be limited by the maximum correction $V_{\text{reg}}\Delta t_{\text{cont}}$ allowed by the shutter velocity V_{reg} (mm/s) (Campisano et al. 2010).

Application

Case Study

The applications of this work concerned the skeletonized WDN (Creaco et al. 2014; Farina et al. 2014) of a town in Northern Italy, the layout of which is shown in Fig. 1. The network consists of 27 nodes (26 nodes with unknown head with ground elevation of 0 m above sea level and 1 source node with ground level of 35 m above sea level) and 32 pipes. Table 1 reports the daily mean nodal demands $\bar{D}$ of network operation, associated with a single consumption category (i.e., domestic). Fig. 2 provides the daily average pattern of the source head and of the multiplying demand coefficient (valid for all the network nodes).

Table 2 reports, for each pipe, the end nodes, length L, diameter D, number $N_{\Delta x}$ of spatial steps used in the discretization for the application of the method of the characteristics, and wall thickness s. In the following calculations, all the pipes were assumed to be made of PVC ($E = 3$ GPa and $n = 0.01$ s/m$^{1/3}$). Eq. (3) is still valid in this case if the viscoelasticity of PVC can be neglected. In fact, strictly speaking, although PVC is a viscoelastic material, its creep deformation is very low compared with other plastic materials (e.g., polyethylene).

Table 1. Demand $\bar{D}$ and Pulse Frequency λ of Network Nodes

Node	$\bar{D}$ (m^3/s)	λ (s^{-1})
1	0.001383	0.197
2	0.000182	0.026
3	0.000920	0.131
4	0.002575	0.366
5	0.002833	0.403
6	0.008358	1.188
7	0.003422	0.486
8	0.005327	0.757
9	0.001521	0.216
10	0.000861	0.122
11	0.002272	0.323
12	0.001313	0.187
13	0.008520	1.211
14	0.000883	0.126
15	0.000216	0.031
16	0.000395	0.056
17	0.000445	0.063
18	0.002817	0.400
19	0.000028	0.004
20	0.000307	0.044
21	0.002597	0.369
22	0.001033	0.147
23	0.001001	0.142
24	0.000531	0.075
25	0.000761	0.108
26	0	0

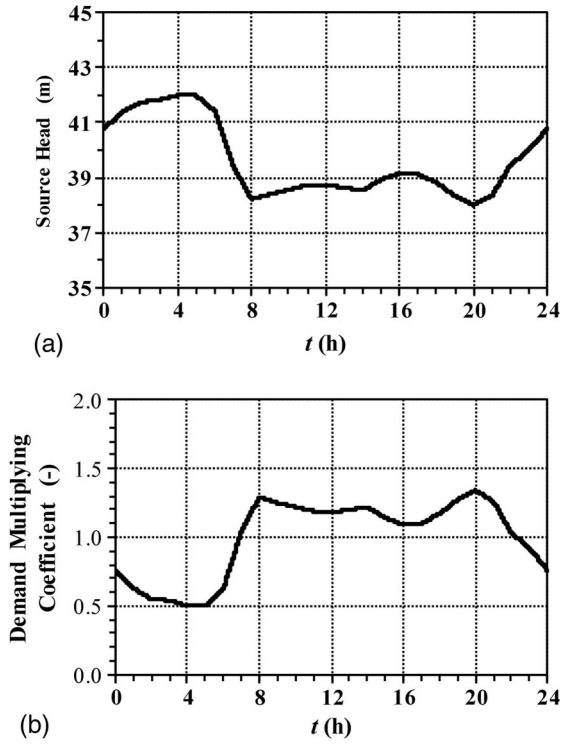

F2:1 **Fig. 2.** Daily pattern of: (a) source head; (b) demand multiplying
F2:2 coefficient

Table 2. Upstream and Downstream Nodes, Length L, Diameter D, Number $N_{\Delta x}$ of Δx in the Discretization and Thickness s for Each Pipe

Pipe	Upstream node	Downstream node	L (m)	D (mm)	$N_{\Delta x}$	s (m)
1	1	2	10.1	100	2	0.006
2	2	3	2,874.5	125	288	0.0075
3	3	4	1,732.8	150	174	0.009
4	1	16	2851.4	125	286	0.0075
5	4	5	2,648.0	200	265	0.012
6	5	7	144.5	200	15	0.012
7	5	6	364.9	200	37	0.012
8	7	10	817.4	150	82	0.009
9	6	13	1,269.8	200	127	0.012
10	7	8	332.7	300	34	0.018
11	8	11	628.3	150	63	0.009
12	9	10	269.7	150	27	0.009
13	11	9	241.3	150	25	0.009
14	8	18	887.8	300	89	0.018
15	12	14	2,055.9	150	206	0.009
16	13	12	130.9	250	14	0.015
17	21	13	991.1	250	100	0.015
18	14	15	6.8	200	1	0.012
19	15	16	607.2	150	61	0.009
20	15	17	1,669.7	125	167	0.0075
21	17	16	1,046.8	150	105	0.009
22	18	21	132.1	300	14	0.018
23	18	19	392.5	450	40	0.027
24	19	20	154.5	450	16	0.027
25	22	23	2,469.3	200	247	0.012
26	22	19	1,593.6	250	160	0.015
27	24	23	2,567.0	125	257	0.0075
28	25	24	2,337.7	100	234	0.006
29	17	25	2,452.7	150	246	0.009
30	27	26	19.6	450	2	0.027
31	26	20	9.6	450	50	0.027
32	20	11	490.9	150	1	0.009

Simulation Framework

The algorithms described in the section Model Structure concerning nodal demand generation, unsteady flow modelling, and RTC were implemented in the *MATLAB* 2016a environment. Calculations were carried out with a laptop with an Intel Core i5-5200 CPU with a frequency of 2.20 GHz and 4 GB of RAM.

The simulation framework did not account for the effects of water discharge and pressure head measurement errors on the effectiveness of RTC. Proof of the stability of RTC in the presence of measurement errors was beyond the scope of the paper and will be investigated in further works. The main objective of this paper was the analysis of the performance of RTC under pulsed demand conditions. The plan of the simulations consisted of

1. Unsteady flow simulation of the network under pulsed demand conditions in the absence of RTC;
2. Unsteady flow simulation of the network under pulsed demand and pressure RTC for the choice of the suitable value of Δt_{cont}; and
3. In the RTC scenario, comparison between the results obtained with the unsteady flow model and those yielded by previous approaches based on EPS modeling.

No data were available in the network to obtain detailed information to estimate the values of the nine parameters (α_T, β_T, T_{min}, T_{max}, α_I, β_I, I_{min}, I_{max}, and ρ) of the bivariate beta distribution for generating correlated pulse durations and intensities for the simulation of the case study network, in which consumption is mainly of domestic kind. Therefore, in the absence of field data for the case study, calibration of the pulse generation model was carried out assuming ~~that~~ the users connected to the selected network nodes to produce pulses with duration and intensity characteristics similar to those provided by Buchberger et al. (2003). This assumption was corroborated by Guercio et al. (2001), who found in Italy similar pulse features to those in Ohio. In the group of 21 households monitored during a 7-month experimental campaign, over 365,000 pulses were observed in Milford, Ohio, with the following statistical characteristics on a continuous time basis during 1 month (Creaco et al. 2017): $\bar{T} = 49$ s, $\bar{I} = 0.0977$ L/s, $\sigma_T = 103.4$ s, $\sigma_I = 0.0665$ L/s, $T_{min} = 0$ s, $I_{min} = 0$ L/s, $T_{max} = 1774$ s, $I_{max} = 0.5101$ L/s, and $\rho = 0.32$. On the basis of these statistics, the nine parameters were estimated for the present case study through the method of the moments. At this stage, a caveat must be made about the chosen values, which may differ from the actual values produced in the network under analysis. Nevertheless, the objective of the work was not to obtain pulses statistically consistent with those of the town selected but rather to obtain realistic pulsed nodal demand to be used in the unsteady flow modeling and to analyze how RTC operated in the presence of pulsed nodal demands. Furthermore, various authors (e.g., Guercio et al. 2001; Creaco et al. 2016b) have noticed that pulse characteristics such as those observed in the Milford households enable accurate residential demand reconstruction in countries different from the United States.

The unsteady flow simulations of the network were performed considering $\Delta t = 0.01$ s. For leakage evaluation through Eq. (5), exponent γ was set to 1, a typical value for plastic pipes (Van Zyl and Cassa 2004). Coefficient α_{leak} was set to 9.4×10^{-9} m/s to obtain a leakage percentage rate of approximately 20% in order to reproduce a realistic estimate relevant to the real system. In Eq. (6), coefficient k_p was set to 0.007, based on the results of Pezzinga (2000). ~~The network pipes have values of ε/D in the range 2×10^{-4} to 1.5×10^{-3}, for which the graphs of Pezzinga (2000) yield values of k_p within the small range 0.005–0.009. Therefore, for simplification purposes, the single value $k_p = 0.007$ was chosen for the whole network.~~

Simulations under RTC were performed assuming a control valve installed downstream of Pipe 32 with End Nodes 26 and 20, in a link with $D = 300$ mm (Fig. 1). In relationship $\xi(\alpha)$ in Eq. (9), coefficients c_1 and c_2 were set to 1.5 and 2.8, respectively (Campisano et al. 2012), which are typical values of needle valves. The RTC algorithm of Creaco and Franchini (2013) was applied considering $K = 1$ in Eq. (10) and valve shutter velocity $V_{reg} = 1$ mm/s, which enables full valve closure from $\alpha = 0$ to $\alpha = 1$ in 300 s. The valve setting α was bounded within the range [0, 0.95]. The target node for the implementation of the selected RTC architecture was chosen according to the procedure proposed by Campisano et al. (2016). Specifically, Node 1 was assumed to be the target node, because it is the node downstream of the control valve with the lowest pressure head. The set point pressure head to achieve at the target node was fixed to 25 m.

Results and Discussion

The parameterization method described in the section Pulsed Demand Generation at Network Nodes [Eq. (2)] yielded the nodal average daily values of λ reported in Table 1. The demand multiplying coefficients in Fig. 2(b) were used to determine an intradaily variation pattern of λ, with 1-s resolution time-step for each node of the network.

The pulse generation model was applied to estimate nodal demands over a 30-day period with 1-s time step for each node of the network. The duration of 30 days was chosen because it ensured

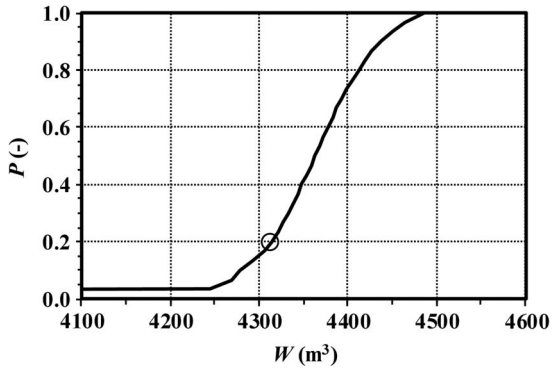

F3:1 **Fig. 3.** Cumulative distribution of daily network water volume W,
F3:2 obtained starting from demand pulses; the circle indicates the water
F3:3 volume value for the day chosen for subsequent calculations

good representativeness of the results in terms of nodal consumption volumes. Furthermore, it is consistent with the time duration in which the mean nodal demands and the trends (Fig. 2) of source head and demand coefficient were estimated. The daily consumption volumes of the network nodes then were re-sorted to obtain the maximum mutual rank correlation, in order to represent a similar behavior for the consumption values of the inhabitants served by the network. Fig. 3 reports the corresponding cumulative distribution of the network daily consumption volume W obtained after re-sorting the daily nodal consumption values. A day with daily demand $W = 4{,}312$ m^3, very close to the average value of 4,366 m^3, was chosen for the subsequent analyses. Figs. 4(a and b) report the time-varying demand in the day and in the morning peak period (from 8 to 9 a.m.), respectively. The graphs clearly show that the obtained trend is much more irregular than that obtained by multiplying the total daily average demand of the network ~~times~~ the demand coefficient reported in Fig. 2(b) (bold line in Fig. 4). Irregularities are ascribed to the presence of pulses-related variations. Fig. 4b shows that demand variations up to approximately ± 8 L/s around the average value can take place during the peak hour due to the stochastic nature of demand pulses.

Fig. 5 presents results of the application of the unsteady flow modelling to the no-RTC scenario. Figs. 5(a and b) report the trend of pressure head h at Critical Node 1 for the whole day simulation and a detail of the time from 8 to 9 a.m., respectively. The two graphs highlight the constant presence of pressure head excess compared to the set point of 25 m with pressure head ranging between 31 and 42 m. This justifies the possibility of obtaining benefits in terms of pressure reduction from the implementation of RTC techniques in the network. Fig. 5b shows that the amplitude of large temporal variations in h within an hour, a result of the stochastic behavior of water demands previously shown in Fig. 4, is up to approximately 3 m (see).

One-hour unsteady flow simulations (time interval: 8–9 a.m.) aimed at choosing the suitable control time step Δt_{cont} for the RTC scenario were carried out for values of $\Delta t_{cont} = 3$, 20, 60, 180, 300, and 600 s. This enabled exploring a range of values larger than the usual range adopted in the practice (normally time steps of a few minutes). Fig. 6 reports results in terms of valve setting α and head h at the target node for $\Delta t_{cont} = 3{,}180$, and 600 s. The RTC system provided slightly improved control as Δt_{cont} decreased from 600 to 180 s. The figure shows that the more frequently the actuator set the corrections, the higher was the

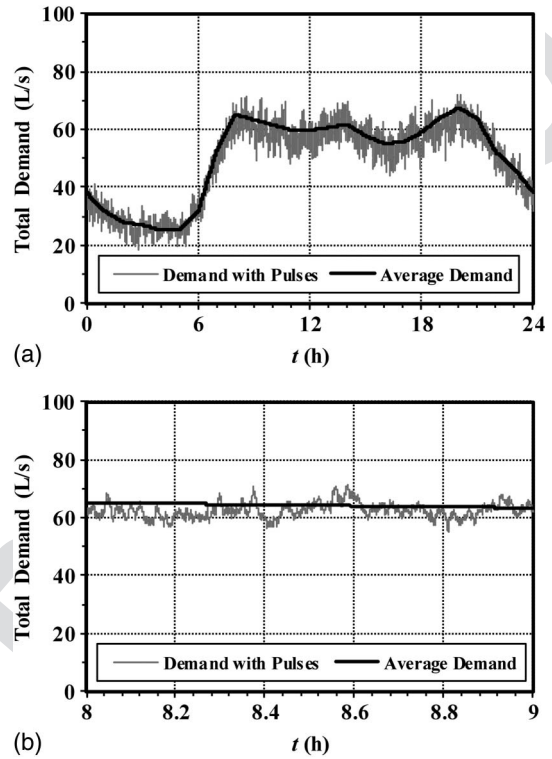

F4:1 **Fig. 4.** Trends of total network demand: (a) in the day selected for
F4:2 the simulations; and (b) from 8 to 9 a.m.; average demand derived
F4:3 from monthly consumption measurements and demand obtained by
F4:4 summing up demand pulses

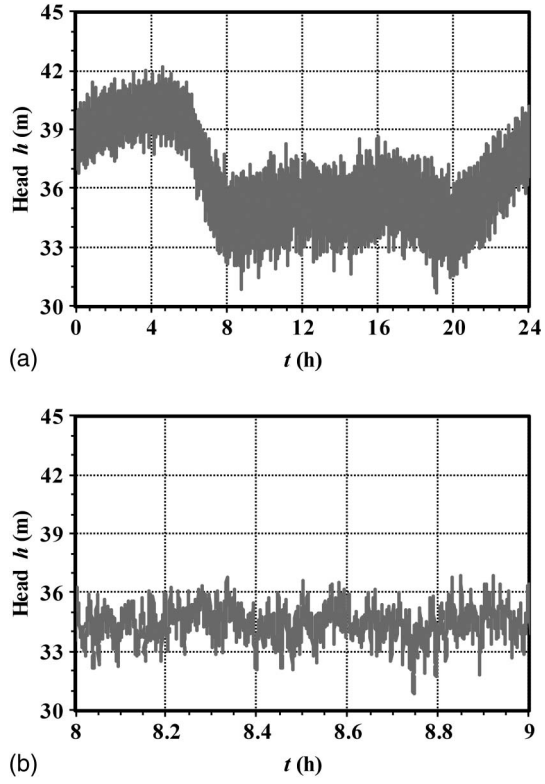

F5:1 **Fig. 5.** Unsteady flow modelling—trend of pressure head h at the
F5:2 critical node in the no-RTC scenario: (a) in the day selected for the
F5:3 simulations; and (b) from 8 to 9 a.m.

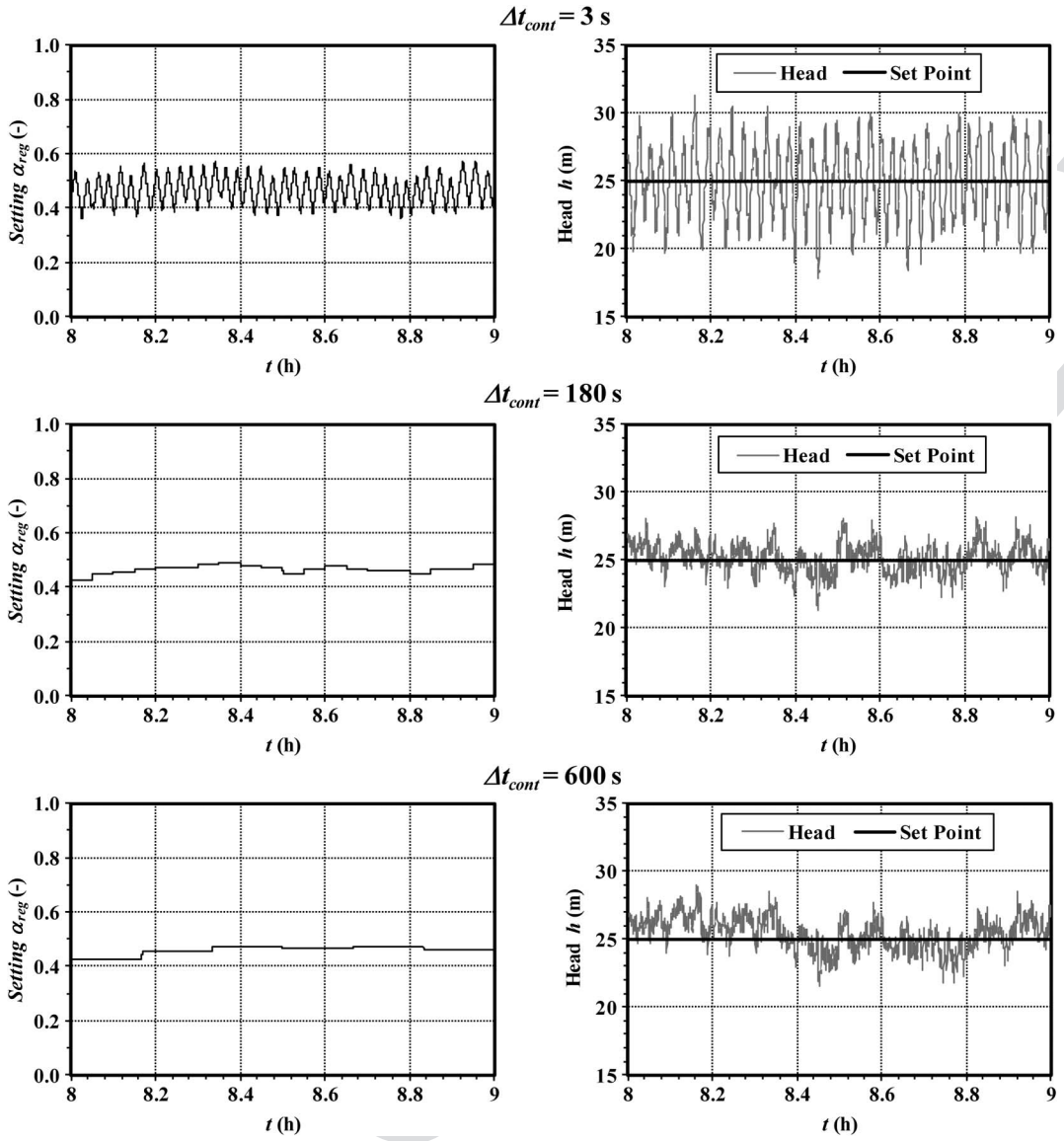

F6:1 **Fig. 6.** For various values of control time step Δt_{cont} in the RTC scenario, valve setting α_{reg} and head h at the critical node from 8 to 9 a.m.

ability of the control system to keep the head close to the set point. However, worse control performance was obtained if overly small values of Δt_{cont} were chosen (i.e., if the control frequency is too high). In fact, for $\Delta t_{\text{cont}} = 3$ s, the RTC algorithm caused a large number of actuator setting corrections and very large deviations of the controlled pressure head from the set point (order of magnitude of 10 m). This behavior, which is consistent with the forecasts of Campisano et al. (2016), occurs because 3 s is too small a time interval for controlling the pressure head at the target node while avoiding instabilities caused by the valve reaction to its own past actions.

In this context, this effect can only be represented through unsteady flow modeling, which, unlike the EPS, enables proper representation of signal propagation in the network. For $\Delta t_{\text{cont}} = 3$, 20, 60, 180, 300, and 600 s, Table 3 reports the average value $|e|_{\text{mean}}$ of absolute deviations $|e|$ and the sum $\Sigma|\Delta\alpha|$ of the actuator setting absolute corrections in the 1-h RTC simulation. Parameter $|e|_{\text{mean}}$ is related to the control effectiveness, whereas $\Sigma|\Delta\alpha|$ provides a measure of the total valve stroke displacements. The higher the value of the two parameters, the lower is the control effectiveness. The table highlights that $\Delta t_{\text{cont}} = 180$ s seems to be a good

Table 3. Average Absolute Deviation $|e|_{\text{mean}}$ and Sum $\Sigma|\Delta\alpha|$ of Absolute Actuator Corrections as a Function of the Regulation Time Step Δt_{cont}

Δt_{cont} (s)	e_{mean} (m)	$\Sigma\lvert\Delta\alpha\rvert$
3	2.23	11.13
20	2.04	5.87
60	0.95	0.68
180	0.86	0.19
300	0.93	0.12
600	1.05	0.07

choice for the network under analysis because it guarantees a good trade-off between closeness of the controlled variable to the set-point (average deviation of 0.86 m) and number of actuator corrections. Accordingly, such a value of Δt_{cont} was chosen for the successive simulation analysis including the adoption of RTC for a 24-h duration. Fig. 7 reports specific results of this analysis. Fig. 7(a) shows the daily trends of α_v and h. The results show that the valve tended to close (high value of α_v) at night and open (low values of α_v) during the day, consistent with the daily pressure

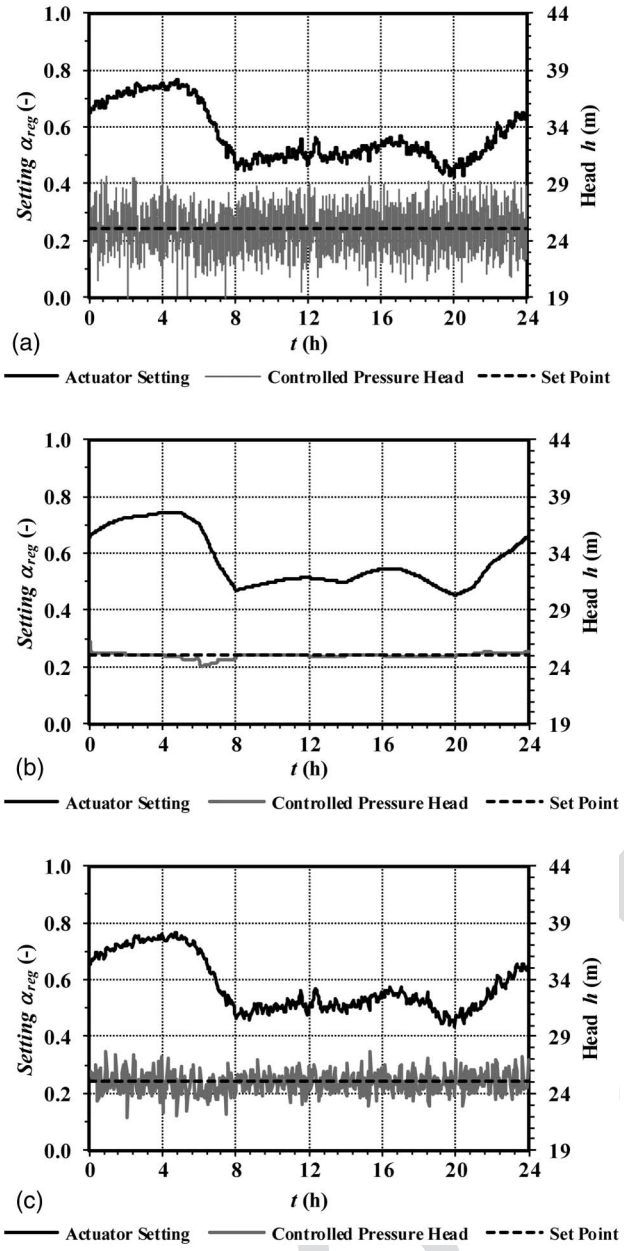

F7:1 **Fig. 7.** Daily trend of actuator setting α_{reg} and of pressure head h at the
F7:2 critical node in the RTC scenario, as obtained in: (a) the unsteady flow
F7:3 simulation; (b) EPS1; (c) EPS2

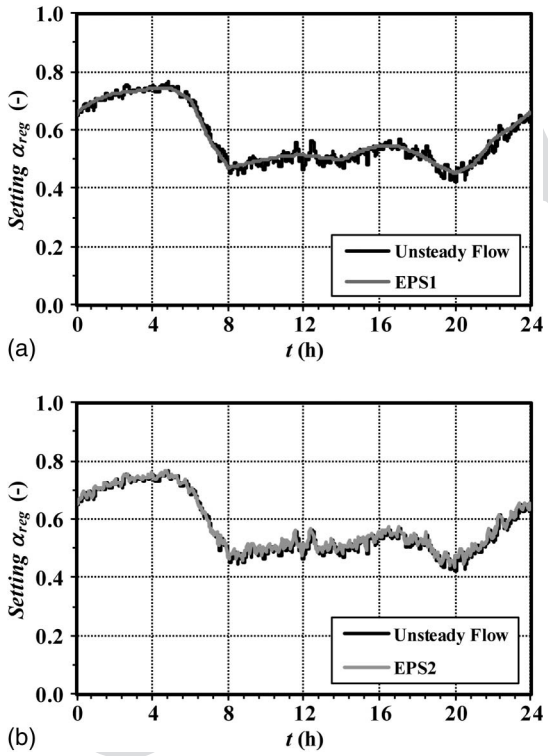

Fig. 8. Daily trend of actuator setting α_{reg} and of pressure head h at the F8:1
critical node in the RTC scenario; comparison of the regulations F8:2
obtained in: (a) unsteady flow modelling and EPS1; and (b) unsteady F8:3
flow modelling and EPS2 F8:4

pattern. On average, h was close to the set-point even if the demand pulse–related pressure head variations caused undershooting down to approximately 22 m and overshooting up to approximately 28 m. However, the presence of pressure undershooting is not believed to create risks of water demand shortfalls in this case.

Globally, Fig. 7(a) shows the capability of the unsteady flow modeling to accurately estimate magnitude and duration of pressure over/undershooting associated with pulsing demands and with hydraulic transients.

Fig. 7 also shows the simulation results obtained by the use of approaches based on EPS. For appropriate comparison with the results of the unsteady flow model, EPS was run using a simulation time step equal to $\Delta t_{cont} = 180$ s, which is sufficiently long to enable transients to be dampened through the network [the basic assumption for the applicability of EPS according to Walski et al. (2003)]. Therefore the source head pattern was obtained by averaging the 1-s time-scale pattern in Fig. 2(a) over time steps of duration Δt_{cont}. Figs. 7(b and c) report the results of two variants of EPS—EPS1 and EPS2, respectively—which differ in the representation of demand. In particular, the EPS1 simulation did not consider the pulsed demand, with nodal demands being obtained using a standard approach [i.e., by multiplying the average nodal demands reported in Table 1 by the pattern reported in Fig. 2(b) and averaging the results over time steps of duration Δt_{cont}]. Approach EPS2 instead used the nodal demands obtained from the aggregation of the pulsed nodal demands used in the unsteady flow modeling over Δt_{cont}.

As expected, the results highlight that the standard EPS version—that is, EPS1 [Fig. 7(b)] —led to inconsistently regular daily trends of α_t and h due to the absence of both pulsed demand modeling and unsteady flow description. Variant EPS2 [Fig. 7(c)] gave more consistent results than did EPS1, although the pressure head variations of EPS2 were smaller than in the unsteady flow modeling. Unsurprisingly, this happened because the pressure head variations of EPS2 were time-averaged over $\Delta t_{cont} = 180$ s.

Fig. 8 gives a more detailed insight into the daily trend of α_t obtained in unsteady flow modeling in EPS1 and EPS2. Fig. 8(a) confirms that EPS1 yielded only a rough temporal average of the valve-setting trend, compared with the unsteady flow modeling. Fig. 8(b) shows that EPS2 yielded good estimates of the temporal variations in the actuator settings. This happened because the RTC algorithm evaluates the actuator corrections through Eq. (10), which considers the temporal average of $e = h - h_{sp}$ over Δt_{cont}. In fact, the unsteady flow modeling and EPS2 gave very close estimates of the temporal average of e, and therefore very close estimates of the temporal variation in α_t.

Summarizing the results of Figs. 7 and 8, some general considerations can be made. The comparison of the approaches highlights that EPS1 yields an oversimplified estimation of pressure heads and valve settings during the day. Nevertheless, because demand pulses and transients do not affect leakage in a significant way, EPS1 can find useful application for a consistent estimate of leakage reduction in RTC scenarios. Instead, a more sophisticated approach, such as EPS2, is required if the analysis of the RTC system control performance is concerned. In fact, approach EPS2 can be suitably used for a good estimate of the behavior of RTC algorithms in terms of time-varying actuator settings. It is necessary to resort to the unsteady flow modeling only in those cases when well-founded estimates of the pressure head variations are needed or when the suitable control time step must be properly defined. In fact, although it accounts for the pulsed nature of demand, EPS2 can underestimate the size of pressure head oscillations by up to 50%. However, the unsteady flow modeling is much more burdensome. In fact, the associated computational time is larger than that of EPS by five orders of magnitude.

Conclusions and Prospects

This paper presented a novel methodology that simulates the remote RTC in WDNs. Unlike most methodologies in the scientific literature, which are based on EPS, it uses the method of the characteristics to model the hydraulic transients associated with demand pulse generation and valve regulations. The applications of the model to a skeletonized real network showed that the RTC unsteady flow simulation gives indications of the amplitude of the actual pressure head variations at the target node. Furthermore, it provides an insight into the choice of the suitable control time step, which should be large enough to enable the signal of the valve setting correction to be sensed by the remotely controlled pressure head. A comparison with the EPS simulation of RTC showed that the latter remains a valid instrument of the first attempt, with much smaller computation times. Specifically, in the absence of the pulsed nodal demands, EPS still can be used for consistent estimates of leakage reductions obtainable from RTC. When temporally aggregated pulsed demands are used as input, EPS can yield very accurate estimates of the temporal variations in the actuator setting and approximate pressured head variations at the controlled node.

Future work will be dedicated to the enhancement of the remote RTC algorithms to reduce the pressure head variations that arise in the WDS when demand pulses are triggered.

Although several studies have been carried out so far to show the benefits of RTC valves in WDNs, an accurate cost/benefit analysis of RTC valves compared with traditional PRVs, including installation and operational costs in the long run, has never been carried out. Therefore future work will be aimed at exploring the extent to which and under which conditions the adoption of RTC for WDN pressure regulation yields benefits compared with traditional PRVs. The analyses of this paper confirmed the stability of RTC, and in particular of the control scheme proposed by Creaco and Franchini (2013), even in the presence of pulsed demand. Another interesting aspect to explore in future works is how RTC reacts in the presence of larger demand changes than those explored in this paper, which are associated with domestic users. In fact, WDNs can experience locally significant demand changes (such as those associated with opening/closing a fire hydrant, a large pipe break, and turning on/off a large in-line booster pump to an adjacent pressure zone), which could cause instability and secondary transients.

References

Ali, M. (2015). "Knowledge-based optimization model for control valve locations in water distribution networks." *J. Water Resour. Plann. Manage.*, 10.1061/(ASCE)WR.1943-5452.0000438, 04014048.

Alvisi, S., Franchini, M., and Marinelli, A. (2003). "~~A stochastic model for representing drinking water demand at residential level~~." *Water Resour. Manage.*, 17(3), 197–222.

Araujo, L. S., Ramos, H., and Coelho, S. T. (2006). "Pressure control for leakage minimisation in water distribution systems management." *Water Resour. Manage.*, 20(1), 133–149.

Berardi, L., and Giustolisi, O. (2016). "Special issue on the battle of background leakage assessment for water networks." *J. Water Resour. Plann. Manage.*, 10.1061/(ASCE)WR.1943-5452.0000667, C2016001.

Berardi, L., Laucelli, D., Ugarelli, R., and Giustolisi, O. (2015). "Leakage management: Planning remote real time controlled pressure reduction in Oppegård municipality." *Procedia Eng.*, 119(1), 72–81.

Buchberger, S. G., Carter, J. T., Lee, Y. H., and Schade, T. G. (2003). "Random demands, travel times and water quality in dead-ends." *AWWARF Rep. No. 294*, AWWARF (American Water Works Association Research Foundation), Denver.

Campisano, A., Creaco, E., and Modica, C. (2010). "RTC of valves for leakage reduction in water supply networks." *J. Water Resour. Plann. Manage.*, 10.1061/(ASCE)0733-9496(2010)136:1(138), 138–141.

Campisano, A., Modica, C., Reitano, S., Ugarelli, R., and Bagherian, S. (2016). "Field-oriented methodology for real-time pressure control to reduce leakage in water distribution networks." *J. Water Resour. Plann. Manage.*, 10.1061/(ASCE)WR.1943-5452.0000697, 04016057.

Campisano, A., Modica, C., and Vetrano, L. (2012). "Calibration of proportional controllers for the RTC of pressures to reduce leakage in water distribution networks." *J. Water Resour. Plann. Manage.*, 10.1061/(ASCE)WR.1943-5452.0000197, 377–384.

Creaco, E., Alvisi, S., and Franchini, M. (2016a). "Multi-step approach for optimizing design and operation of the C-Town pipe network model." *J. Water Resour. Plann. Manage.*, 10.1061/(ASCE)WR.1943-5452.0000585, C4015005.

Creaco, E., Blokker, M., and Buchberger, S. (2017). "~~Models for generating household water demand pulses: Literature review and comparison~~." *J. Water Resour. Plann. Manage.*, ~~10.1061/(ASCE)WR.1943-5452.0000763~~.

Creaco, E., Farmani, R., Kapelan, Z., Vamvakeridou-Lyroudia, L., and Savic, D. (2015). "Considering the mutual dependence of pulse duration and intensity in models for generating residential water demand." *J. Water Resour. Plann. Manage.*, 10.1061/(ASCE)WR.1943-5452.0000557, 04015031.

Creaco, E., and Franchini, M. (2013). "A new algorithm for the real time pressure control in water distribution networks." *Water Sci. Technol. Water Supply*, 13(4), 875–882.

Creaco, E., Franchini, M., and Walski, T. M. (2014). "Accounting for phasing of construction within the design of water distribution networks." *J. Water Resour. Plann. Manage.*, 10.1061/(ASCE)WR.1943-5452.0000358, 598–606.

Creaco, E., Kossieris, P., Vamvakeridou-Lyroudia, L., Makropoulos, C., Kapelan, Z., and Savic, D. (2016b). "Parameterizing residential water demand pulse models through smart meter readings." *Environ. Modell. Software*, 80, 33–40.

Creaco, E., and Pezzinga, G. (2015a). "Embedding linear programming in multi objective genetic algorithms for reducing the size of the search space with application to leakage minimization in water distribution networks." *Environ. Modell. Software*, 69(C), 308–318.

Creaco, E., and Pezzinga, G. (2015b). "Multi-objective optimization of pipe replacements and control valve installations for leakage attenuation in water distribution networks." *J. Water Resour. Plann. Manage.*, 10.1061/(ASCE)WR.1943-5452.0000458, 04014059.

Farina, G., Creaco, E., and Franchini, M. (2014). "Using EPANET for modelling water distribution systems with users along the pipes." *Civil Eng. Environ. Syst.*, 31(1), 36–50.

Farley, M., and Trow, S. (2003). *Losses in water distribution networks*, IWA (International Water Association), London.

Germanopoulos, G., and Jowitt, P. W. (1989). "Leakage reduction by excessive pressure minimization in a water supply network." *Proc. Inst. Civil Eng.*, 2(87), 195–214.

Guercio, R., Magini, R., and Pallavicini, I. (2001). "Instantaneous residential water demand as stochastic point process." *Water resources management*, C. A. Brebbia, et al., eds., WIT Press, Southampton, U.K., 129–138.

Hall, A. R. (2004). "Generalized method of moments." *Advanced texts in econometrics*, Oxford University Press, Oxford.

Iman, R. L., and Canover, W. J. (1982). "A distribution-free approach to inducing rank correlation among input variables." *Commun. Stat.*, 11(3), 311–334.

Jung, B. S., and Karney, B. (2009). "Systematic surge protection for worst-case transient loadings in water distribution systems." *J. Hydraul. Eng.*, 10.1061/(ASCE)0733-9429(2009)135:3(218), 218–223.

Liberatore, S., and Sechi, G. M. (2009). "Location and calibration of valves in water distribution networks using a scatter-search meta-heuristic approach." *Water Resour. Manage.*, 23(8), 1479–1495.

McInnis, D., and Karney, B. (1995). "Transients in distribution networks: Field tests and demand models." *J. Hydraul. Eng.*, 10.1061/(ASCE)0733-9429(1995)121:3(218), 218–231.

Nault, J. D., and Karney, B. W. (2016). "Adaptive hybrid transient formulation for simulating incompressible pipe network hydraulics." *J. Hydraul. Eng.*, 10.1061/(ASCE)HY.1943-7900.0001195, 04016050.

Nicolini, M., and Zovatto, L. (2009). "Optimal location and control of pressure reducing valves in water networks." *J. Water Resour. Plann. Manage.*, 10.1061/(ASCE)0733-9496(2009)135:3(178), 178–187.

Pezzinga, G. (1999). "Quasi-2D model for unsteady flow in pipe networks." *J. Hydraul. Eng.*, 10.1061/(ASCE)0733-9429(1999)125:7(676), 676–685.

Pezzinga, G. (2000). "Evaluation of unsteady flow resistances by quasi-2D or 1D models." *J. Hydraul. Eng.*, 10.1061/(ASCE)0733-9429(2000)126:10(778), 778–785.

Prescott, S. L., and Ulanicki, B. (2008). "Improved control of pressure reducing valves in water distribution networks." *J. Hydraul. Eng.*, 10.1061/(ASCE)0733-9429(2008)134:1(56), 56–65.

Streeter, V., Wylie, E. B. W., and Bedford, K. W. (1998). *Fluid mechanics*, 9th Ed., McGraw-Hill, New York.

Svrcek, W. Y., Mahoney, D. P., and Young, B. R. (2014). *A real-time approach to process control*, Wiley, Mississauga, Canada.

Ulanicki, B., and Skworcow, P. (2014). "Why PRVs tends to oscillate at low flows." *Procedia Eng.*, 89, 378–385.

Vairavamoorthy, K., and Lumbers, J. (1998). "Leakage reduction in water distribution systems: Optimal valve control." *J. Hydraul. Eng.*, 10.1061/(ASCE)0733-9429(1998)124:11(1146), 1146–1154.

Van Zyl, J. E., and Cassa, A. M. (2014). "Modeling elastically deforming leaks in water distribution pipes." *J. Hydraul. Eng.*, 140(2), 182–189.

Vicente, D., Garrote, L., Sánchez, R., and Santillán, D. (2016). "Pressure management in water distribution systems: Current status, proposals, and future trends." *J. Water Resour. Plann. Manage.*, 10.1061/(ASCE)WR.1943-5452.0000589, 04015061.

Walski, M., Chase, D., Savic, D., Grayman, W., Beckwith, S., and Koelle, E. (2003). *Advanced water distribution modelling and management*, Haestad, Waterbury, CT.

Wylie, E. B., Streeter, V. L., and Suo, L. (1993). *Fluid transients in systems*, Prentice Hall, Englewood Cliffs, NJ.

Zhang, Q., Karney, B., and Pejovic, S. (2011). "Nonreflective boundary design via remote sensing and proportional-integral-derivative control valve." *J. Hydraul. Eng.*, 10.1061/(ASCE)HY.1943-7900.0000403, 1477–1489.

Queries

1. Please provide the ASCE Membership Grades for the authors who are members.

2. Please provide department for “Univ. of Adelaide” for affiliation footnote 1.

3. (ASCE Open Access: Authors may choose to publish their papers through ASCE Open Access, making the paper freely available to all readers via the ASCE Library website. ASCE Open Access papers will be published under the Creative Commons-Attribution Only (CC-BY) License. The fee for this service is $1750, and must be paid prior to publication. If you indicate Yes, you will receive a follow-up message with payment instructions. If you indicate No, your paper will be published in the typical subscribed-access section of the Journal.)

4. Please check the hierarchy of section heading levels.

5. ASCE style requires full reference details for the software "MATLAB”. Please provide the full details for (ABAQUS), and we will insert it in the References list and link it to this citation.

6. The citation Van Zyl and Cassa (2004) mentioned in this sentence is not present in the References list. Please provide the full details and we will insert it in the References list and link it to this citation.

7. This query was generated by an automatic reference checking system. Reference Alvisi et al. (2003) could not be located in the databases used by the system. While the reference may be correct, we ask that you check it so we can provide as many links to the referenced articles as possible.

8. This query was generated by an automatic reference checking system. Reference Creaco et al. (2017) could not be located in the databases used by the system. While the reference may be correct, we ask that you check it so we can provide as many links to the referenced articles as possible.

9. Please provide page range for Creaco et al. (2017).

10. Please provide issue number for Creaco et al. (2016b).

11. This query was generated by an automatic reference checking system. Reference Creaco et al. (2016b) could not be located in the databases used by the system. While the reference may be correct, we ask that you check it so we can provide as many links to the referenced articles as possible.

12. COMP: This reference has been moved from its original position. Pease update the links.

13. A check of online databases year found in this reference. Please Add year ’2007’.

14. This query was generated by an automatic reference checking system. Reference Van Zyl and Cassa (2014) could not be located in the databases used by the system. While the reference may be correct, we ask that you check it so we can provide as many links to the referenced articles as possible.